THE JOURNAL OF PHYSICAL CHEMISTRY B

Article

pubs.acs.org/JPCB

Electron Transport in Supported and Tethered Lipid Bilayers Modified with Bioelectroactive Molecules

Rui Campos and Ritu Kataky*

Department of Chemistry, Durham University, South Road, Durham, DH1 3LE, United Kingdom

Supporting Information

ABSTRACT: Tethered bilayer lipid membranes (tBLMs) are commonly used as model membranes. However, in biophysical studies, free-standing membranes ("black" lipid membranes) are more realistic models of cellular processes. In this article, we discuss the rates of electron transfer in both types of bilayer lipid membranes. These BLMs were then modified using two very important mitochondrial membrane-associated molecules: ubiquinone-10 (UQ_{10}) and α-tocopherol (VitE). The electron transfer rates in the unmodified films were studied with three redox couples, $Fe(CN)_6^{3-/4-}$, $Ru(NH_3)_6^{3+/2+}$, and NAD^+/NADH, using electrochemical impedance spectroscopy (EIS) and cyclic voltammetry (CV). The rate of electron transfer in the modified films was studied using the biologically relevant NAD^+/NADH electroactive couple using the same methods. It is shown that when the BLMs are modified with only UQ_{10}, it is possible to observe electron transfer. However, when the antioxidant VitE is added to the modification, the electron transfer provided by UQ_{10} is inhibited. Following initial studies using CV, a comparison of electron transfer theory and data was used to investigate this phenomenon in more detail, using EIS data. The standard rate constant caused by electron tunneling across the film, k_{th}^0, depends on the value of β used. Two different values of the potential independent electron tunneling coefficient, β, were fitted, and it is shown that a β value half of those usually reported in literature (refereed here as β_{app}) gives better agreement between the theory and the experimental results. The unmodified films present k_{th}^0 values on the order of 10^{-15} cm s^{-1} when $\beta = 0.72$ Å^{-1} and k_{th}^0 values on the order of 10^{-9} cm s^{-1} when $\beta_{app} = 0.38$ Å^{-1}. For the modified films, the values of k_{th}^0 are on the order of 10^{-15} cm s^{-1} when $\beta = 0.72$ Å^{-1} and 10^{-9} cm s^{-1} for $\beta_{app} = 0.38$ Å^{-1}. The experimental electron transfer rate constant, k_{app}^0, is on the order of 10^{-8} cm s^{-1} for unmodified and modified (with (i) UQ_{10}, (ii) VitE, and (iii) UQ_{10} + VitE) films.

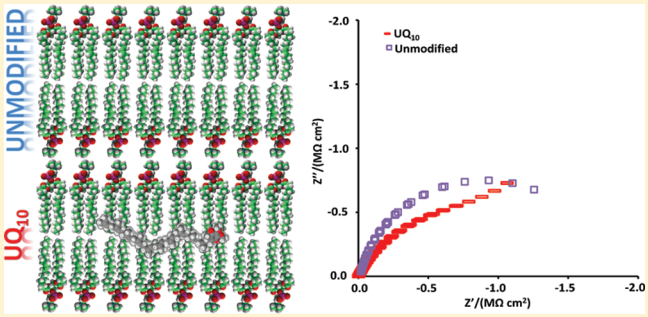

1. INTRODUCTION

Bilayer lipid membranes (BLMs) are widely used to mimic the cell membrane[1−5] and are used to study transport phenomena and other forms of cell signal transduction.[6−8] There are many ways of preparing BLMs, each one with its advantages and disadvantages: tethered BLMs (tBLMs) are veryc robust and stable,[2−4,6,9] and the main advantage of black lipid membranes (also known as free-standing BLMs between two aqueous solutions) is that the membrane is formed between two aqueous solutions, which makes it a better mimic of the cell membrane.[1,4] In black lipid membranes, electrodes are inserted in two aqueous phases separated by the BLM, which allows the measurement of the membrane potential and the rate of electron transport.[10−12] In the tBLMs, the lower leaflet (self-assembled monolayer) is formed by chemisorption of the thiolipid or alkanethiol on a gold surface.[13−15] These chemisorbed structures inspire considerable interest in electrochemistry because of their potential for testing the Marcus model of electron transfer[16,17] and for the study of electron transfer in BLMs.[16,18] To understand the various electron transport mechanisms, the self-assembled monolayers (SAMs) need to be sufficiently compact so that electrochemical processes occurring directly at the gold-solution interface are suppressed.[17,19] In addition, the quality of the BLM is dependent on the quality of the SAM.[17,20]

In previous reports, black lipid membranes have been used to study electron transport[10,21] and ion transport[11,12,22] and have been incorporated into microfluidic devices.[23,24] In electron transport studies, Shiba et al[10] modified psBLMs with 7,7,8,8-tetracyanoquinodimethane and decamethyl ferrocene and studied the electron transfer between $[Fe(CN)_6]^{4-}$ in one phase and $[Fe(CN)_6]^{3-}$ in the other. They concluded that the electron transport can occur by two distinct mechanisms: either by an electron-hopping mechanism in which electron transport is facilitated by the redox species in the BLM or it is controlled by mass transfer of the redox species. Cliffel and co-workers[21] used SECM to measure mass transport of $Ru(NH_3)_6Cl_3$ in phosphatidylcholine bilayer lipid membranes modified with alamethicin pores.

Received: October 11, 2011
Revised: February 24, 2012
Published: March 1, 2012

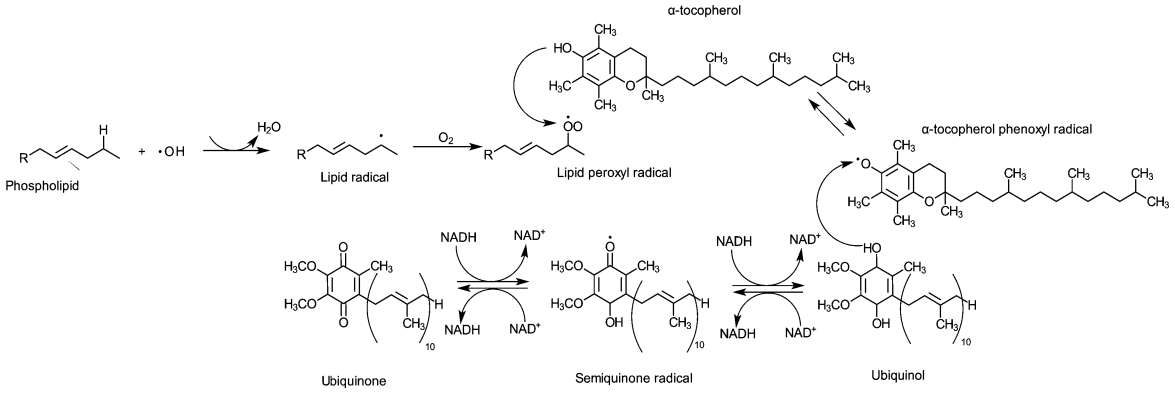

Figure 1. Interaction between the lipids, VitE and UQ_{10}.[35−40]

In relevant ion transport studies, Ozaki and co-workers demonstrated that an uncoupler, carbonylcyanide *p*-trifluoromethoxyphenylhydrazone, inserted in a black lipid membrane can induce pH-dependent transport of H^+ and Na^+ in the absence of ion channels or ion carriers.[12] The transport of Li^+, Na^+, K^+, and NH_4^+ has been studied using different ion channels and ion carriers, where is shown a dependence of ion transport on the amount of ion channel/ion carrier.[11]

Proof of principle for the formation of black lipid membranes suitable for incorporation in microfluidic devices has bedn reported by several groups; however, these publications do not report any mechanistic studies.

In this paper, we chose to study the effects on electron transport rates of two very important mitochondrial membrane-associated molecules, ubiquinone-10 (UQ_{10}) and α-tocopherol (VitE), using both tBLMS and black lipid membranes (in our case, the membrane support is a micropore array and, therefore, termed pore-suspended BLMs, psBLMs) using three redox couples: $Fe(CN)_6^{3-/4-}$, $Ru(NH_3)_6^{3+/2+}$, and NAD^+/NADH.

The most important role of mitochondria is to produce adenosine triphosphate (ATP) through respiration and to regulate cellular metabolism in the Kreb's cycle.[25] Within the mitochondria, UQ_{10} is particularly interesting because of its central role in the electron transfer chain.[26−28] UQ_{10} has a 10 unit isoprenoid (5 nm) semirigid chain, and because of this, its most likely position within the lipid bilayer is in the membrane midplane.[26,29,30] α-Tocopherol (VitE) is the most likely vitamin to react with UQ_{10} because both are redox-active, lipophilic compounds present in the membrane and both have antioxidant properties.[31]

VitE consists of a chroman head and a phytyl tail.[32] Its position in the bilayer is not completely clear, and three positions have been suggested: (i) the tail is well within the hydrophobic domain of the bilayer, but the chroman head is placed near the water−lipid interface; (ii) the chroman head is around 1 nm away from the interface; and (iii) the molecule is well within the hydrophobic region of the membrane bilayer.[30]

UQ_{10} protects cell membranes from oxidation by reacting with lipid radicals produced in the lipid peroxidation chain reaction. The reduced form of UQ_{10} can react with the oxidized VitE, reactivating its redox active capabilities.[28,33,34] VitE scavenges peroxide free radicals and converts them to less toxic lipid hydroperoxides. The phenoxyl radical of VitE reacts with ubiquinol to reactivate its antioxidant properties (Figure 1).[35−40]

In previous work, Schiffrin and co-workers studied self-assembled monolayers on mercury electrodes,[26] confirming that the phospholipid monolayer modified with UQ_{10} showed redox chemistry. The redox process was shown to be dependent on the position of the quinone headgroup, and for pH > 7, the incorporation of UQ_{10} in the monolayer made its reduction very irreversible. At pH < 7, the reaction followed a disproportionation route involving the ubiquinone radical. In contrast to this report, Marchal and co-workers[41] studied laterally supported dimyristoyl phosphatidylcholine BLMs inserted with UQ_{10} on a microporous electrode and found that below pH 12, the two electrons/two protons electrochemical process at the gold electrode appeared under kinetic control, and they based all their thermodynamic deductions on the observed reversibility of the quinone/hydroquinol anion transformation at pH > 13. Schiffrin et al.[27] also studied transmembrane electron transfer across phospholipid bilayer membranes (BLMs) mediated by ubiquinone, using patch clamp micropipets. They used Fe(II)/Fe(III) citrate solutions to control redox potentials and reported a transfer coefficient of 0.5. They concluded that the rate-determining step is the transfer of the semiubiquinone radical anion, instead of charge transfer reactions at the membrane/electrolyte solution boundaries.

Transmembrane electron transfer reactions have been studied by Hurst et al.[42,43] and by Hammarström et al.[44,45] Hurst's group studied electron transfer across bilayer membranes of dihexadecyl phosphate in small unilamellar vesicles containing viologen (*N*,*N*′-dialkyl-4,4′-bipyridinium). They observed that violgen radicals inserted in the membrane phase could mediate electron transfer. They concluded that short-chain (<12 C units) viologens act as mobile relays, whereas long-chain viologens transfer electrons mainly by electron tunneling. However, using phosphatidylcholine vesicles with viologen radicals as the external electron donor and $Fe(CN)_6^{3-}$ as the internal electron acceptor, Hammarström and co-workers have shown that the transfer through the phospholipid membrane is preceded by disproportionation of the viologen radical to the neutral form, and the mechanism for electron transfer is transport, and not tunneling.

In our work, all the measurements were made at pH 7.4 to mimic the physiological conditions. We used NAD^+/NADH as electron mediators for mimicking biological systems. The redox reaction of NAD^+/NADH involves the transfer of two electrons and has been used to study biological phenomena, processes involving chemical transformation, and energy conversion and enzymatic reactions.[46]

2. EXPERIMENTAL SECTION

2.1. Reagents and Chemicals. Potassium ferrocyanide ($K_4Fe(CN)_6$), potassium ferricyanide ($K_3Fe(CN)_6$), hexaammineruthenium(III) chloride ($Ru(NH_3)_6Cl_3$), hexaammineruthenium(II)

dx.doi.org/10.1021/jp209772u | J. Phys. Chem. B 2012, 116, 3909−3917

chloride ($Ru(NH_3)_6Cl_2$), L-α-phosphatidylcholine (EggPC), β-nicotinamide adenine dinucleotide reduced disodium salt hydrate (NADH), β-nicotinamide adenine dinucleotide hydrate (NAD^+), 4-(2-hydroxyethyl)piperazine-1-ethanesulfonic acid (HEPES), and *n*-decane were purchased from Sigma-Aldrich, UK. 1,2-Dipalmitoyl-*sn*-glycerophosphothioethanol (DPPTE) was purchased from Avanti Polar Lipids, USA. Hydrogen peroxide and sulphuric acid were obtained from Acros Organics and Fluka, respectively. Solvents were used without further purification. HEPES buffer solution (HEPES/NaOH, pH 7.4[47]) was prepared using deionized water (Sartorius Arium 611 ultrapure water system (resistivity of not less than 18.2 MΩ cm). All the other solutions were prepared in HEPES buffer.

2.2. Instrumentation. A potentiostat-galvanostat model PGSTAT12 (Autolab) interfaced with a personal computer was used for the electrochemical impedance spectroscopy (EIS) measurements. ZPlot software was used to interpret the raw impedance data. A three-electrode cell containing Ag/AgCl (3.5 M KCl); Pt foil (A = 1 cm^2); and either bare gold electrode, SAM, or BLM electrodes were employed as reference, auxiliary, and working electrodes, respectively. The cell was placed in a Faraday cage to eliminate external interference. All potentials in this work are reported with respect to Ag/AgCl (3.5 M KCl). All measurements were carried out at room temperature. The Nyquist and Bode plots were fitted, according to literature precedent,[48−50] using a modified Randles circuit, which takes into account a frequency-dependent constant phase element (CPE) instead of the double layer capacitance to account for topological imperfections of the gold electrode and of the membrane.

2.3. Preparation of Organic Solution of Lipids. A stock solution, 20 mg mL^{-1} of DPPTE, was made by dissolving the lipid in chloroform to prevent oxidation.[51] To prepare the working solution, the chloroform solution of lipid (either EggPC or a mixture of DPPTE and EggPC) was placed in a glass vial and dried under a slow stream of argon. The thin lipid film formed was dissolved in *n*-decane.

2.4. Formation of tBLM. *2.4.1. Substrate Preparation.* The formation of a monolayer on gold is strongly dependent on the cleanliness and structure of the gold prior to modification.[52,53] Polycrystalline gold electrodes were used rather than single-crystal Au electrodes as they are more readily available, and previous literature has shown that properly prepared surfaces are adequate for these studies, provided the constant phase element is close to unity.[54] Gold is a soft metal and is readily contaminated by organic and inorganic species; therefore, prior to monolayer preparation, the gold substrates were well cleaned to remove the contaminants on the surface that affect the integrity of the SAM formation. In this work, polycrystalline gold disk electrodes (Au(111)) (BAS, area 0.020 cm^2) were polished for 60 s in a figure-eight pattern on Buhler Microcloth with successively finer grades (15, 6, 3, and 1 μm) of diamond polish slurries and alumina slurry (0.05 μm), followed by sonication in ethanol and water for 10 min. Immediately before use, polycrystalline gold electrodes were cleaned by soaking in piranha solution (3:1 (v/v) 98% H_2SO_4/30% H_2O_2) for 20 min; rinsed with water; and finally, dried under argon. (*Caution: piranha solution is a vigorous oxidant and should be handled very carefully.*)

2.4.2. Preparation of Vesicles. A chloroform solution of EggPC, or lipid with UQ_{10}, VitE, or both was dried in a glass vial under a slow stream of argon to yield a thin lipid film. The vial was placed in vacuum overnight to ensure that all solvent had been removed. The dried lipid was hydrated at room temperature using HEPES buffer solution, resulting in multilamellar vesicles. To obtain small unilamellar vesicles, the hydrated lipid was sonicated for 20 min.

2.4.3. BLM Deposition. SAMs were formed by dipping the gold electrode in a *n*-decane solution of 1 mM DPPTE and 0.5 mM of EggPC, or lipids and UQ_{10} (0.02 mM) or VitE (0.02 mM) (or both)[26,27,55] (Figure 2), for 24 h at room temperature.[20,53,56−58] DPPTE molecules chemisorb to the gold surface via the thiol group. EggPC was used to fill possible gaps between the DPPTE molecules, leading to a better quality SAM.[20] The SAM produced serves as the lower leaflet of the BLM.

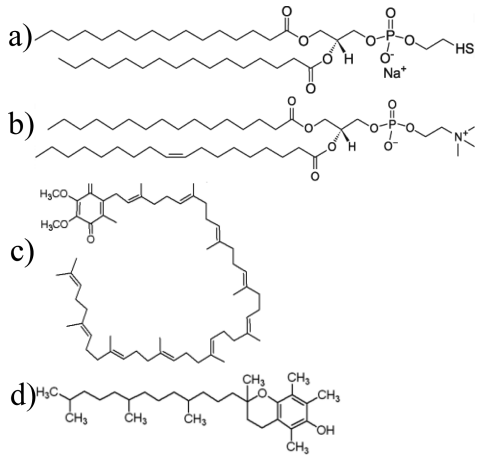

Figure 2. Structure of (a) DPPTE, (b) EggPC, (c) ubiquinone-10, and (d) α-tocopherol.

After SAM formation, the electrodes were rinsed with *n*-decane and water to remove weakly attached lipids and dried using argon. The electrodes were transferred to the previously prepared vesicle solution. The bilayer was formed within a few hours.

2.5. Formation of BLM between Two Aqueous Solutions (psBLM). The psBLM was formed on a micropore array that consisted of 8 micropores with a diameter of 50 ± 3 μm (Figure 3).[59] The psBLM was obtained by placing 20 μL

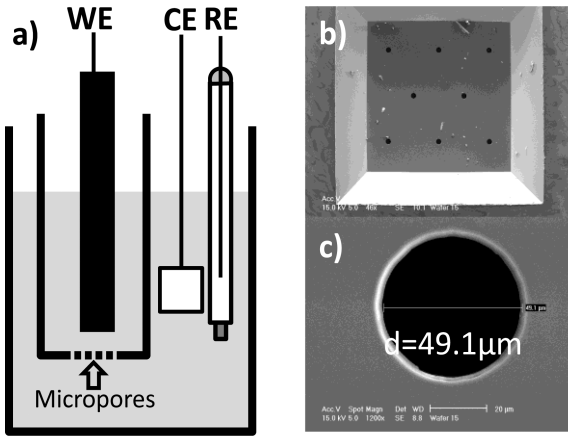

Figure 3. (a) Schematic representation of the experimental setup for the psBLM. The psBLM was deposited on the micropores, and it was between the working and the reference and counter electrodes. (b) Top view of the micropore array; the eight pores are arranged in a hexagonal pattern. (c) One of the pores of the array. The diameter is 50 ± 3 μm.

dx.doi.org/10.1021/jp209772u | J. Phys. Chem. B 2012, 116, 3909−3917

of a 1 mg/mL *n*-decane solution of EggPC, or lipid with UQ_{10} (0.02 mM) or VitE (0.02 mM) (or both), in the micropore array. After drying, an additional 20 μL of the same solution was placed on the other side of the micropore array. The psBLM was formed when both sides of the micropore array came into contact with an aqueous solution.[60]

2.6. Cyclic Voltammetry Measurements. The blocking properties of the films were examined using cyclic voltammetry. The measurements were performed in HEPES buffer solutions (pH 7.4)[47] containing one of the following electroactive couples: $Fe(CN)_6^{3-/4-}$, $Ru(NH_3)_6^{3+/2+}$and $NAD^+/NADH$. In the case of the psBLMs, the measurements were performed in a normal three electrode system, with the working electrode (Au, 0.020 cm^2) being placed in one side of the psBLM and the reference (Ag/AgCl, 3.5 M KCl) and counter (Pt flag, 1 cm^2) being placed on the other side of the psBLM (Figure 3).[7,61−64] Both chambers were filled with the same working solution.

2.7. Electrochemical Impedance Spectroscopy Measurements. EIS is a very powerful technique for estimating kinetic parameters and the structural integrity of mono- and bilayers.[17,18,60] The AC impedance method is based upon a measurement of the response of the electrochemical cell to a small perturbation at the equilibrium potential and monitoring the phase shift of the current response over a range of frequencies. Impedance measurements were made at the equilibrium potential of the redox couples, $Fe(CN)_6^{3-/4-}$ ($E^{0\prime}$ = +0.225 V vs SCE), $Ru(NH_3)_6^{3+/2+}$ ($E^{0\prime}$ = −0.180 V vs SCE), or $NAD^+/NADH$ ($E^{0\prime}$ = −0.560 vs SCE), at a wide range of frequencies from 1.0×10^{-5} to 0.1 Hz, with a perturbation of 10 mV in the potential. The electrolyte solution contained 1 mM of $Fe(CN)_6^{3-/4-}$, 1 mM of $Ru(NH_3)_6^{3+/2+}$, or 0.5 mM of $NAD^+/NADH$ and HEPES buffer solution, background.

3. RESULTS AND DISCUSSION

3.1. Unmodified Films. The first characterization of the films was made using CV. The redox reaction is completely inhibited, indicating that the film formed is well organized and pinhole-free (data not shown).

The formation of the BLMs was determined by its charge transfer resistance and capacitance values. These values were obtained by fitting the Nyquist plots shown in Figure 4 with a modified Randles circuit (Figure 4d), which takes into account a frequency-dependent constant phase element (CPE), to the EIS data.

Previous reports indicate that well formed BLMs, tBLMs, and supported BLMs should present a capacitance in the range 0.4−0.8 μF cm^{-2},[18,27,51,58,65] and its charge transfer resistance should be in the range 10^5−$10^7\Omega$ cm^2.[9,57,60,65−67] In our studies, for all the electroactive species, tBLMs showed a normalized capacitance of 0.41−0.44 ± 0.03 μF cm^{-2}, whereas psBLMs showed values between 0.41 and 0.47 ± 0.03 μF cm^{-2}; the charge transfer resistance values, for both types of BLMs, are in the megaohm centimeter square region (Table 1). All the values fall within the values previously reported, indicating that the structures formed are BLMs.

3.2. Modified Films. Initially, the characterization of the modified films (with UQ_{10}, VitE, and a mixture of UQ_{10} and VitE) was carried out using CV. Only films modified with UQ_{10} showed evidence of electron transfer, (Figures S1−S3 in the Supporting Information). However, CV investigations were complicated by the possible formation of adsorbants due to the $NAD^+/NADH$ (Figure S4 in Supporting Information). We avoided the use of artificial mediators to mimic the biochemical system. Further analysis of data was complicated using CV; therefore, we resorted to impedance spectroscopy for quantitative analyses.

When the modification of the films was made only with UQ_{10}, the charge transfer resistance decreased to 0.85 ± 0.02 MΩ cm^2 in the case of the tBLMs and 0.22 ± 0.02 MΩ cm^2 for the psBLMs. This can be attributed to the fact that UQ_{10}, which is hydrophobic, sits in the membrane midplane and facilitates electron transport and redox reactions.[27] The Nyquist plots showed a small, straight line at low frequencies (Figure 5), indicating a mass transfer control region and, thus, faradic charge transfer.

In contrast, when VitE was used in the modification of the films, the charge transfer resistance increased[68] (0.38 ± 0.02 MΩ cm^2 for the tBLMs and 0.05 ± 0.01 MΩ cm^2 in the case of the psBLMs). It is interesting to note that the increment was smaller (0.12 ± 0.01 MΩ cm^2 for the tBLMs and 0.02 ± 0.01 MΩ cm^2 for the psBLMs) when an equimolar mixture of VitE and UQ_{10} was used to make the modification (Table 2). Another interesting point is that for the films that were modified with the equimolar mixture of VitE and UQ_{10}, the electron transfer due to UQ_{10} was fully suppressed (the Nyquist plots show a semicircle in the entire frequency region, Figure 5). This was attributable to the antioxidant functions of VitE.[33,68,69]

3.3. Electron Transfer Kinetics. The charge transfer kinetics and the existence of defects caused by collapse of monolayers, which influences the electron transfer kinetics and the quality of the BLM, was further analyzed. A comparison of electron transfer theory and data was used to investigate this phenomenon in more detail using EIS data.[16,18,70,71]

If there are no pinholes in the SAM/BLM, the mechanism for electron transfer is tunneling across the film.[16,18,70,71] In this case, the faradic current should, at any potential, decrease exponentially with the film thickness according to the equation[72]

$$i = i_0 \exp(-\beta d) \tag{1}$$

where i_0 is the current measured at bare electrode, d is the thickness of the film, and β is the potential independent electron tunneling coefficient. The parameter β is a measure of the magnitude of current lost per unit length of each molecule, which can vary from ∼0 $Å^{-1}$ for metals to 3.5 $Å^{-1}$ close to vacuum.[73,74]

From eq 1, it is possible to deduce that the standard rate constant caused by electron tunneling across the film, k^0_{th}, should also be dependent on the thickness of the film[18,71]

$$k^0_{th} = k^0_b \exp(-\beta d) \tag{2}$$

where k^0_b is the standard electron transfer rate constant (0.031 cm s^{-1} for the redox couple $Fe(CN)_6^{3-/4-}$,[70] 0.40 cm s^{-1} for the couple $Ru(NH_3)_6^{3+/2+}$,[71] and 0.1 cm s^{-1} for the couple $NAD^+/NADH$[46]). The value of d used in eqs 1 and 2 is given by[18]

$$d = \frac{\varepsilon\varepsilon_r}{C_{layer\ ocp}} \tag{3}$$

where ε is the vacuum permittivity (8.85×10^{-14} F cm^{-1}), ε_r is the relative dielectric constant within the hydrocarbon region of the BLM (2.08 when *n*-decane is the solvent[75]), and $C_{layer\ ocp}$ is the normalized membrane capacitance.

The thickness, d, of the SAMs was to be about∼ 2 nm, approximately one-half the thickness of both tBLMs and psBLMs (Table 3). These values are in good agreement with

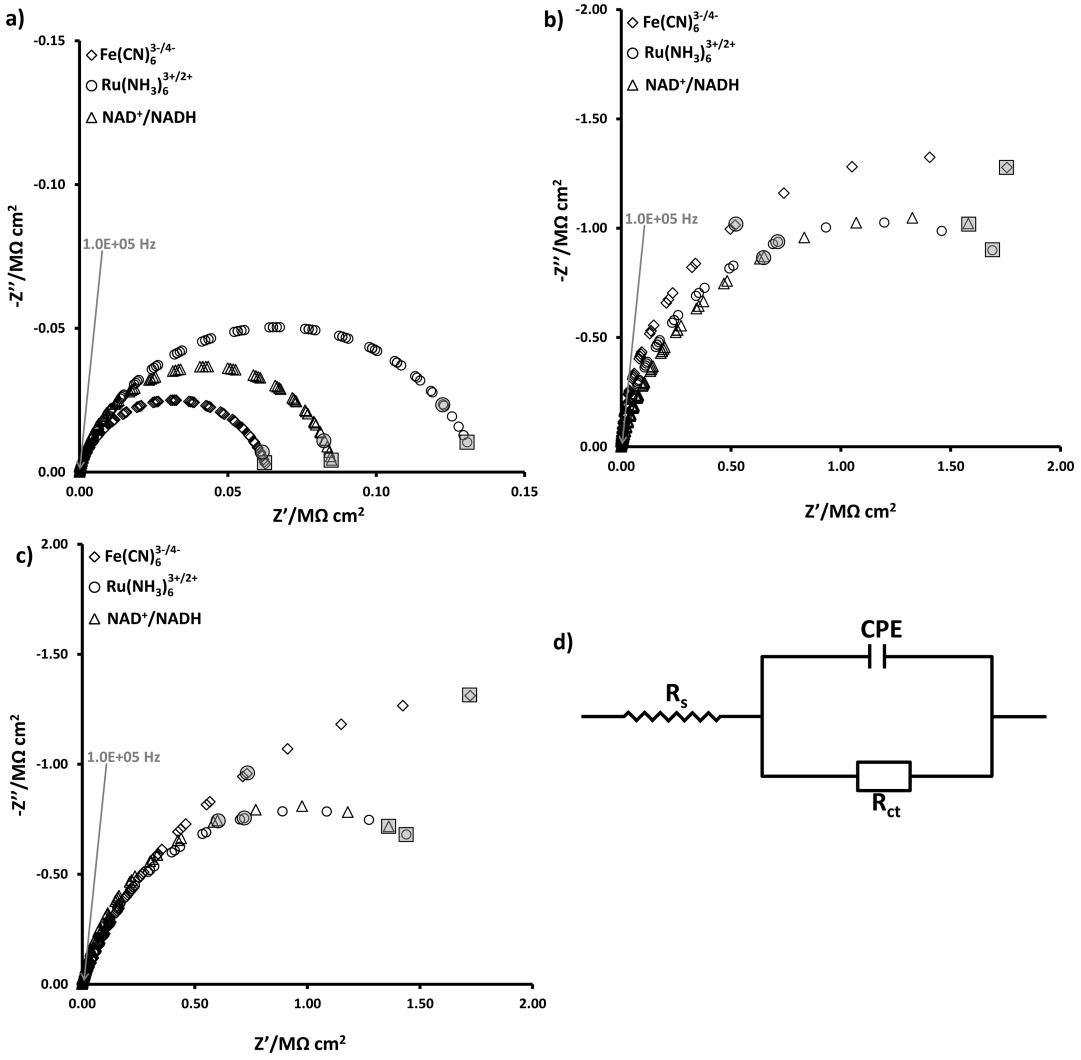

Figure 4. Nyquist plots for the unmodified films: (a) SAM, (b) tBLM, (c) psBLM, and (d) equivalent circuit used to fit the data of the unmodified films. The semicircle in the entire frequency range indicates that the electron transfer reaction is completely inhibited. Although the R_{ct} in the SAMs is quite disperse, that is not noticeable in the tBLM. The lipids present in the second layer of the tBLM corrected possible defects in the SAM, making it a more uniform film.[20] The measurements were made between 1.0×10^5 and 0.1 Hz, at the open circuit potential of each of the electroactive couples. $[Fe(CN)_6^{3-/4-}] = [Ru(NH_3)_6^{3+/2+}] = 1$ mM; $[NAD^+/NADH] = 0.5$ mM, HEPES buffer solution as background. The spectrum points inside a circle correspond to a frequency of 0.3 Hz, and the spectrum points inside a square correspond to 0.1 Hz.

Table 1. Normalized capacitance and Charge Transfer Resistance of the Unmodified Films Formed in This Work[a]

		$C_{layer\ ocp}/(\mu F\ cm^{-2})$	$R_{ct}/(M\Omega\ cm^2)$
$Fe(CN)_6^{3-/4-}$	SAM	1.12 ± 0.10	0.06 ± 0.01
	tBLM	0.43 ± 0.03	2.80 ± 0.22
	psBLM	0.43 ± 0.03	3.74 ± 0.32
$Ru(NH_3)_6^{3+/2+}$	SAM	0.95 ± 0.09	0.13 ± 0.01
	tBLM	0.41 ± 0.03	2.32 ± 0.20
	psBLM	0.41 ± 0.03	1.95 ± 0.18
$NAD^+/NADH$	SAM	0.90 ± 0.08	0.09 ± 0.01
	tBLM	0.44 ± 0.03	2.22 ± 0.17
	psBLM	0.47 ± 0.04	1.90 ± 0.17

[a]The values here presented indicate that the structures formed are mono- and bilayers.

the values reported by Fettiplace[75] and Diao,[18] who reported values of 4 nm. The thickness of the modified films is presented in Table 4. The apparent electron transfer rate constant, k^0_{app}, can be interpreted as representing the effect of defects on electron transfer rate. Using EIS measurements at open circuit potentials (ocp), k^0_{app} is defined as[70]

$$k^0_{app} = \frac{RT}{n^2F^2cR_{ct}A} \quad (4)$$

where R is the gas constant, T is the temperature, F is the Faraday constant, c is the concentration of the redox couple, R_{ct} is the charge transfer resistance, and A is the geometric area of the electrode. The charge transfer resistance was extracted from EIS data by fitting the data with an equivalent circuit included in the ZPLOT software, taking into account the CPE.

We used two different values of β when calculating the standard rate constant caused by electron tunneling across the film, k^0_{th}. In the first set of calculations, we used a value of $\beta = 0.72$ Å^{-1}, which was previously used by Diao and his co-workers for probing electron transfer on Pt-BLMs[18] using $K_3Fe(CN)_6$ as the probe molecule, although the value is never explicitly shown or mentioned. When using this value of β in our work, it yielded values of k^0_{th} on the order of 10^{-15} cm s^{-1}

dx.doi.org/10.1021/jp209772u | J. Phys. Chem. B 2012, 116, 3909–3917

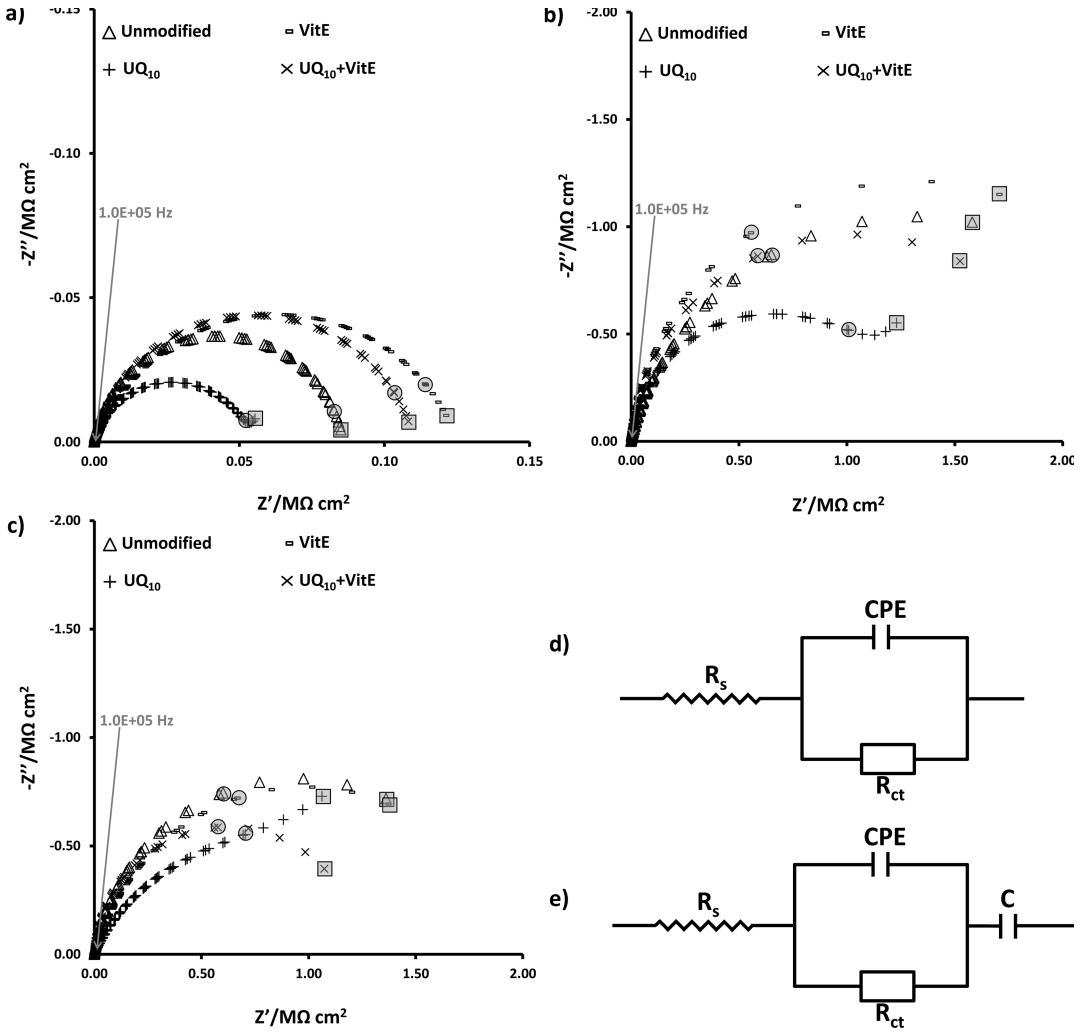

Figure 5. Nyquist plots for (a) SAM; (b) tBLM; (c) psBLM modified with UQ_{10} and VitE; (d) equivalent circuit used to fit the data of unmodified films, films modified with VitE and modified with an equimolar mixture of UQ_{10} and VitE; and (e) equivalent circuit used to fit the data of the films modified only with UQ_{10}. When the modification was made only with UQ_{10}, it was possible to observe a mass transfer control region at low frequencies; in all the other cases, only kinetic control was observed. This means that when the films were modified only with UQ_{10}, there was electron transfer, and in the other cases, the electron transfer was inhibited. The measurements were made between 1.0×10^5 and 0.1 Hz at the open circuit potential of the electroactive couple. [NAD^+/NADH] = 0.5 mM, HEPES buffer solution as background. The spectra points inside a circle correspond to a frequency of 0.3 Hz, and the spectra points inside a square correspond to 0.1 Hz.

Table 2. Normalized Capacitance and Charge Transfer Resistance of the Films Modified with UQ_{10}, VitE and a Mixture of Both[a]

		$C_{layer\ ocp}/(\mu F\ cm^{-2})$	$R_{ct}/(M\Omega\ cm^2)$
SAM	unmodified	0.90 ± 0.08	0.09 ± 0.01
	UQ_{10}	0.97 ± 0.08	0.05 ± 0.01
	VitE	0.91 ± 0.08	0.12 ± 0.01
	UQ_{10} + VitE	0.93 ± 0.08	0.11 ± 0.01
tBLM	unmodified	0.44 ± 0.03	2.22 ± 0.17
	UQ10	0.47 ± 0.04	1.37 ± 0.15
	VitE	0.43 ± 0.03	2.60 ± 0.25
	UQ_{10} + VitE	0.43 ± 0.03	2.34 ± 0.23
psBLM	unmodified	0.47 ± 0.04	1.90 ± 0.17
	UQ_{10}	0.50 ± 0.05	1.68 ± 0.16
	VitE	0.45 ± 0.04	1.95 ± 0.19
	UQ_{10} + VitE	0.47 ± 0.04	1.92 ± 0.18

[a]The values here presented indicate that the structures formed were mono- and bilayers.

for the bilayers which, when compared with k^0_{app}, gives differences over 6 orders of magnitude (Table 3), which are clearly incorrect. However, in the case of the SAMs formed with a mixture of DPPTE and EggPC, the values obtained are in accordance with previous literature.[70,76,77] For the modified films, the range of differences between k^0_{th} and k^0_{app} is, like for unmodified films, over 6 orders of magnitude (Table 4).

We then tried a different approach. The value of β used was based on the conclusions that Mirkin and co-workers reached when studying electron transfer through lipid monolayers at a liquid/liquid interface.[78] They have shown that, as a result of penetration of $ZnPor^+$ into the lipid monolayer, β is about one-half of that usually reported (β_{app}). Assuming that in our case there is also penetration of the redox couple into the lipid bilayer, the value of β_{app} used was 0.38 $Å^{-1}$. Using this β_{app}, the difference between k^0_{th} and k^0_{app} is reduced to less than 2 orders of magnitude (Tables 3 and 4).

The differences between k^0_{th} and k^0_{app} can be explained only when assuming that the electroactive couple ions diffuse through

dx.doi.org/10.1021/jp209772u | J. Phys. Chem. B 2012, 116, 3909–3917

Table 3. Thickness, Apparent Electron Transfer Rate Constant and Standard Rate Constant Caused by Tunneling for the Different Unmodified Films[a]

			k_{th}^0/(cm s^{-1})		
		d/nm	β = 0.72 Å^{-1}	β_{app} = 0.38 Å^{-1}	k_{app}^0/(cm s^{-1})
$Fe(CN)_6^{3-/4-}$	SAM	1.7 ± 0.2	(1.45 ± 0.15) × 10^{-7}		(4.13 ± 0.32) × 10^{-6}
	tBLM	4.3 ± 0.4	(8.56 ± 0.85) × 10^{-16}	(2.16 ± 0.20) × 10^{-9}	(9.36 ± 0.85) × 10^{-8}
	psBLM	4.3 ± 0.4	(1.05 ± 0.10) × 10^{-15}	(2.42 ± 0.24) × 10^{-9}	(6.99 ± 0.54) × 10^{-8}
$Ru(NH_3)_6^{3+/2+}$	SAM	2.0 ± 0.2	(2.08 ± 0.20) × 10^{-7}		(1.94 ± 0.19) × 10^{-6}
	tBLM	4.9 ± 0.5	(2.64 ± 0.25) × 10^{-16}	(3.89 ± 0.40) × 10^{-9}	(1.13 ± 0.13) × 10^{-7}
	psBLM	4.4 ± 0.4	(5.26 ± 0.50) × 10^{-15}	(1.89 ± 0.17) × 10^{-8}	(1.34 ± 0.13) × 10^{-7}
NAD^+/NADH	SAM	2.1 ± 0.2	(3.85 ± 0.39) × 10^{-8}		(1.52 ± 0.15) × 10^{-6}
	tBLM	4.2 ± 0.4	(9.88 ± 1.00) × 10^{-15}	(1.37 ± 0.14) × 10^{-8}	(5.91 ± 0.59) × 10^{-8}
	psBLM	4.0 ± 0.4	(4.43 ± 0.40) × 10^{-14}	(3.02 ± 0.30) × 10^{-8}	(6.89 ± 0.70) × 10^{-8}

[a]The thickness of the films is around 2 nm for a SAM and around 4.5 nm for the bilayers.

Table 4. Thickness, Apparent Electron Transfer Rate Constant and Standard Rate Constant Caused by Tunneling for the Different Modified Films[a]

			K_{th}^0/(cm s^{-1})		
		d/nm	β = 0.72 Å^{-1}	β_{app} = 0.38 Å^{-1}	k_{app}^0/(cm s^{-1})
SAM	unmodified	2.1 ± 0.2	(3.85 ± 0.38) × 10^{-8}		(1.52 ± 0.15) × 10^{-6}
	UQ_{10}	1.9 ± 0.2	(1.11 ± 0.10) × 10^{-7}		(2.41 ± 0.24) × 10^{-6}
	VitE	2.0 ± 0.2	(4.82 ± 0.48) × 10^{-8}		(1.05 ± 0.10) × 10^{-6}
	UQ_{10} + VitE	1.9 ± 0.2	(6.04 ± 0.60) × 10^{-8}		(1.19 ± 0.12) × 10^{-6}
tBLM	unmodified	4.2 ± 0.4	(9.88 ± 1.00 × 10^{-15}	(1.37 ± 0.14) × 10^{-8}	(5.91 ± 0.60) × 10^{-8}
	UQ_{10}	3.9 ± 0.4	(6.97 ± 0.70) × 10^{-14}	(3.84 ± 0.38) × 10^{-8}	(9.54 ± 1.00) × 10^{-8}
	VitE	4.3 ± 0.4	(3.66 ± 0.37) × 10^{-15}	(8.10 ± 0.80) × 10^{-9}	(5.04 ± 0.50) × 10^{-8}
	UQ_{10} + VitE	4.2 ± 0.4	(5.21 ± 0.52) × 10^{-15}	(9.76 ± 1.00) × 10^{-9}	(5.60 ± 0.56) × 10^{-8}
psBLM	unmodified	4.0 ± 0.4	(4.43 ± 0.44) × 10^{-14}	(3.02 ± 0.30) × 10^{-8}	(6.89 ± 0.70) × 10^{-8}
	UQ_{10}	3.7 ± 0.4	(2.57 ± 0.26) × 10^{-13}	(7.65 ± 0.77) × 10^{-8}	(7.81 ± 0.78) × 10^{-8}
	VitE	4.1 ± 0.4	(2.01 ± 0.20) × 10^{-14}	(1.99 ± 0.20) × 10^{-8}	(6.72 ± 0.67) × 10^{-8}
	UQ_{10} + VitE	3.9 ± 0.4	(6.24 ± 0.62) × 10^{-14}	(3.62 ± 0.36) × 10^{-8}	(6.83 ± 0.68) × 10^{-8}

[a]The thickness of the films is around 2 nm for a SAM and around 4 nm for the bilayers.

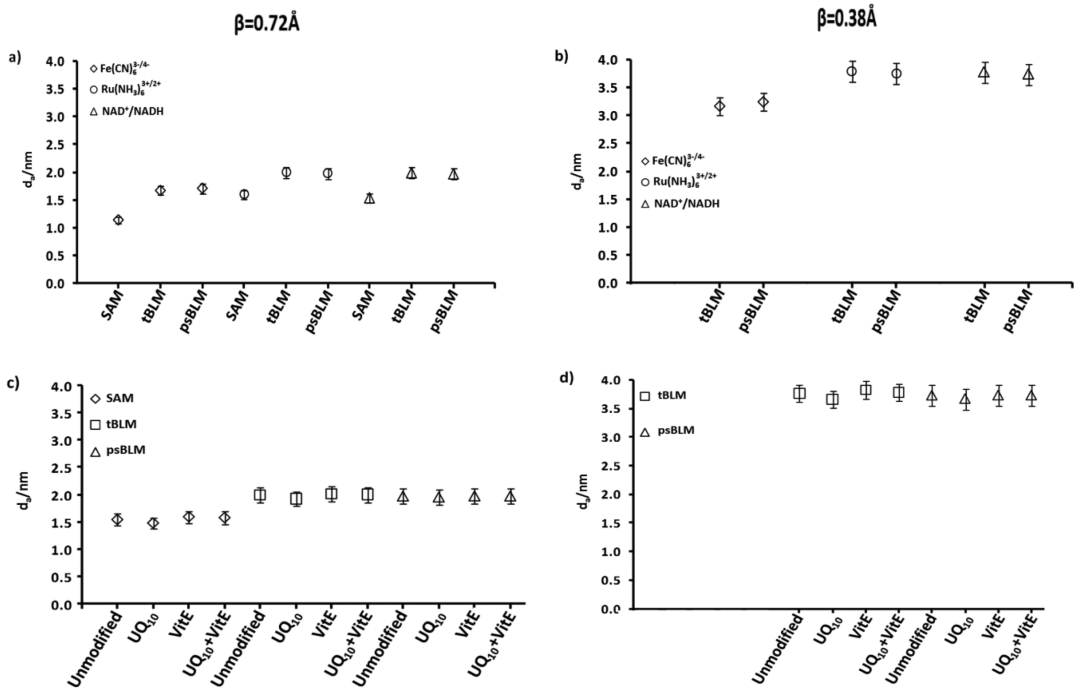

Figure 6. Representation of d_a for the different films and different modifications for θ_a = 1. Parts a and b are the unmodified films with β = 0.72 Å^{-1} and 0.38 Å^{-1}, respectively. Parts c and d are the modified films with β = 0.72 Å^{-1} and 0.38 Å^{-1}, respectively.

dx.doi.org/10.1021/jp209772u | J. Phys. Chem. B 2012, 116, 3909−3917

defects in the structure formed; electron transfer occurs via a tunneling process across a relatively thin film.[17] The diffusion through the thin film is the rate-limiting step; otherwise, the Nyquist plots would not show only a semicircle[17] for the faradic charge transfer, as observed in the films modified with UQ_{10}.

Assuming that all defects in the mono- or bilayers formed are independent and applying the same mathematical treatment to eq 1 as shown in previous publications,[70,76] the average fractional film coverage, θ_a, can be defined as

$$\theta_a = \frac{\left(\frac{k^0_{app}}{k^0_b} - \exp(-\beta d_0)\right)}{\exp(-\beta d_a) - \exp(-\beta d_0)} \quad (5)$$

where d_a is the average film thickness of a well assembled monolayer or bilayer and all the other parameters have the same meaning as before.

The average fractional film coverage gives an estimate of the presence of defects in the film. When $\theta_a = 1$, d_a represents the average film thickness. If d_a is close to d_0, that means that the film is quasi-defect-free.[70,76]

A comparison between the values presented in Figure 6 a and b and the values in Table 4 reveals that the difference between d_a and d_0 for the SAMs is around 4 Å. This range of differences has been reported in the case of alkylated Au electrodes,[70] and in the case of the bilayers, the differences are in the range of 20–23 Å for $\beta = 0.72$ Å^{-1} and around 4 Å when $\beta_{app} = 0.38$ Å^{-1}.

4. CONCLUSION

Electron transfer across phospholipid monolayers and bilayers (SAM, tBLM, and psBLM) were measured using EIS spectroscopy using three different probe molecules. The capacitance and resistance presented in this work were consistent with previously reported values. We did not observe any significant differences between inner- ($Fe(CN)_6^{3-/4-}$) and outer- ($Ru(NH_3)_6^{3+/2+}$) sphere electron transfer mechanisms or between these and the biological cofactor NAD^+/NADH.

The analysis and fitting of the experimental values (using a modified Randles circuit, which takes into account a frequency dependent constant phase element (CPE) instead of the double-layer capacitance to account for topological imperfections of the gold electrode and of the film membrane) to the theoretical values led us to use two different values of the potential independent electron tunneling coefficient. We found that the difference between the apparent and the standard rate constants caused by electron tunneling is much smaller when β is close to one-half of that previously reported (β_{app}), as previously shown by Mirkin and Bard.[78] We, therefore, conclude that β_{app} for electron tunneling through a phospholipid bilayer is on the order of 0.38 Å^{-1}.

In addition, the kinetics of electron transfer across phospholipid monolayers and bilayers mediated by UQ_{10} was measured as 10^{-6} cm s^{-1} for monolayers and 10^{-8} cm s^{-1} for bilayers. Electron transfer does not occur when the films are modified with VitE or mixture of VitE and UQ_{10}.

Both pore-suspended and supported films are essentially porous films; therefore, we have found that the same pore model that is used to analyze electron transfer in SAMs and tBLMs is applicable for psBLMs.

■ ASSOCIATED CONTENT

Supporting Information

Cyclic voltammograms of all the films modified with UQ_{10}, VitE, and an equimolar mixture of UQ_{10} and VitE are presented. This material is available free of charge via the Internet at http://pubs.acs.org/.

■ AUTHOR INFORMATION

Corresponding Author

*E-mail: ritu.kataky@durham.ac.uk.

Notes

The authors declare no competing financial interest.

■ ACKNOWLEDGMENTS

This work was funded by EPSRC.

■ REFERENCES

(1) Tien, H. T.; Ottova, A. L. *J. Membr. Sci.* **2001**, *189*, 83–117.
(2) Sackmann, E. *Science* **1996**, *271*, 43–48.
(3) Koper, I. *Mol. Biosyst.* **2007**, *3*, 651–657.
(4) Castellana, E. T.; Cremer, P. S. *Surf. Sci. Rep.* **2006**, *61*, 429–444.
(5) von Heijne, G.; Rees, D. *Curr. Opin. Struct. Biol.* **2008**, *18*, 403–405.
(6) Plant, A. L. *Langmuir* **1993**, *9*, 2764–2767.
(7) Tien, H. T.; Ottova, A. L. *Colloids Surf., A* **1999**, *149*, 217–233.
(8) Junghans, A.; Koper, I. *Langmuir* **2010**, *26*, 11035–11040.
(9) Janshoff, A.; Steinem, C. *Anal. Bioanal.Chem.* **2006**, *385*, 433–451.
(10) Shiba, H.; Maeda, K.; Ichieda, N.; Kasuno, M.; Yoshida, Y.; Shirai, O.; Kihara, S. *J. Electroanal. Chem.* **2003**, *556*, 1–11.
(11) Favero, G.; D'Annibale, A.; Campanella, L.; Santucci, R.; Ferri, T. *Anal. Chim. Acta* **2002**, *460*, 23–34.
(12) Ozaki, S.; Shirai, O.; Kihara, S.; Kano, K. *Electrochem. Commun.* **2007**, *9*, 2266–2270.
(13) Lang, H.; Duschl, C.; Vogel, H. *Langmuir* **1994**, *10*, 197–210.
(14) Vallejo, A. E.; Gervasi, C. A. *Bioelectrochemistry* **2002**, *57*, 1–7.
(15) Cannes, C.; Kanoufi, F.; Bard, A. J. *J. Electroanal. Chem.* **2003**, *547*, 83–91.
(16) Krysinski, P.; Zebrowska, A.; Palys, B.; Lotowski, Z. *J. Electrochem. Soc.* **2002**, *149*, E189–E194.
(17) Diao, P.; Jiang, D.; Cui, X.; Gu, D.; Tong, R.; Zhong, B. *Bioelectrochem. Bioenerg.* **1999**, *48*, 469–475.
(18) Diao, P.; Jiang, D.; Cui, X.; Gu, D.; Tong, R.; Zhong, B. *Bioelectrochem. Bioenerg.* **1998**, *45*, 173–179.
(19) Finklea, H. O.; Avery, S.; Lynch, M.; Furtsch, T. *Langmuir* **1987**, *3*, 409–413.
(20) Jadhav, S. R.; Sui, D.; Garavito, R. M.; Worden, R. M. *J. Colloid Interface Sci.* **2008**, *322*, 465–472.
(21) Wilburn, J. P.; Wright, D. W.; Cliffel, D. E. *Analyst* **2006**, *131*, 311–316.
(22) Shirai, O.; Yoshida, Y.; Kihara, S.; Ohnuki, T.; Uehara, A.; Yamana, H. *J. Electroanal. Chem.* **2006**, *595*, 53–59.
(23) Sandison, M. E.; Zagnoni, M.; Abu-Hantash, M.; Morgan, H. *J. Micromech. Microeng.* **2007**, *17*, S189–S196.
(24) Malmstadt, N.; Nash, M. A.; Purnell, R. F.; Schmidt, J. J. *Nano Lett.* **2006**, *6*, 1961–1965.
(25) Lehninger, A.; Nelson, D.; Cox, M. *Lehninger Principles of Biochemistry*; 5th ed.; W. H. Freeman: New York, 2008.
(26) Gordillo, G. J.; Schiffrin, D. J. *Faraday Discuss.* **2000**, *116*, 89–107.
(27) Cheng, Y.; Cunnane, V. J.; Kontturi, A.-K.; Kontturi, K.; Schiffrin, D. J. *J. Phys. Chem.* **1996**, *100*, 15470–15477.
(28) Crane, F. L.; Sun, I. L.; Barr, R.; Löw, H. *J. Bioenerg. Biomembr.* **1991**, *23*, 773–803.
(29) Söderhäll, J. A.; Laaksonen, A. *J. Phys. Chem. B* **2001**, *105*, 9308–9315.

(30) Afri, M.; Ehrenberg, B.; Talmon, Y.; Schmidt, J.; Cohen, Y.; Frimer, A. A. *Chem. Phys. Lipids* **2004**, *131*, 107−121.
(31) Constantinescu, A.; Maguire, J. J.; Packer, L. *Mol. Aspects Med.* **1994**, *15* (Supplement 1), s57−s65.
(32) Kamal-Eldin, A.; Appelqvist, L.-Å. *Lipids* **1996**, *31*, 671−701.
(33) Traber, M. G.; Atkinson, J. *Free Radical Biol. Med.* **2007**, *43*, 4−15.
(34) Urano, S.; Iida, M.; Otani, I.; Matsuo, M. *Biochem. Biophys. Res. Commun.* **1987**, *146*, 1413−1418.
(35) Kagan, V.; Fabisiak, J.; Quinn, P. *Protoplasma* **2000**, *214*, 11−18.
(36) May, J. M. *Front. Biosci.* **1998**, *2*, d1−10.
(37) Mukai, K.; Itoh, S.; Morimoto, H. *J. Biol. Chem.* **1992**, *267*, 22277−22281.
(38) Stocker, R.; Keaney, J. F. *Physiol. Rev.* **2004**, *84*, 1381−1478.
(39) Gille, L.; Rosenau, T.; Kozlov, A. V.; Gregor, W. *Biochem. Pharmacol.* **2008**, *76*, 289−302.
(40) Gregor, W.; Staniek, K.; Nohl, H.; Gille, L. *Biochem. Pharmacol.* **2006**, *71*, 1589−1601.
(41) Marchal, D.; Boireau, W.; Laval, J. M.; Moiroux, J.; Bourdillon, C. *Biophys. J.* **1997**, *72*, 2679−2687.
(42) Lymar, S. V.; Hurst, J. K. *J. Am. Chem. Soc.* **1992**, *114*, 9498−9503.
(43) Patterson, B. C.; Thompson, D. H.; Hurst, J. K. *J. Am. Chem. Soc.* **1988**, *110*, 3656−3657.
(44) Hammarstroem, L.; Almgren, M.; Lind, J.; Merenyi, G.; Norrby, T.; Aakermark, B. *J. Phys. Chem.* **1993**, *97*, 10083−10091.
(45) Hammarstroem, L.; Almgren, M.; Norrby, T. *J. Phys. Chem.* **1992**, *96*, 5017−5024.
(46) Elving, P. J.; Bresnahan, W. T.; Moiroux, J.; Samec, Z. *Bioelectrochem. Bioenerg.* **1982**, *9*, 365−378.
(47) Dawson, R. M. C.; Elliott, D. C.; Elliott, W. H.; Jones, K. M. *Data for Biochemical Research*; Oxford University Press, Inc: New York, 1986.
(48) Xing, Y. F.; Li, S. F. Y.; Lau, A. K. H.; O'Shea, S. J. *J. Electroanal. Chem.* **2005**, *583*, 124−132.
(49) Shon, Y.-S.; Colorado, R.; Williams, C. T.; Bain, C. D.; Lee, T. R. *Langmuir* **2000**, *16*, 541−548.
(50) Schmitt, E. K.; Weichbrodt, C.; Steinem, C. *Soft Matter* **2009**, *5*, 3347−3353.
(51) Naumowicz, M.; Figaszewski, Z. *Bioelectrochemistry* **2003**, *61*, 21−27.
(52) Yang, M.; Zhang, Z. *Electrochim. Acta* **2004**, *49*, 5089−5095.
(53) Vockenroth, I. K.; Fine, D.; Dodobalapur, A.; Jenkins, A. T. A.; Köper, I. *Electrochem. Commun.* **2008**, *10*, 323−328.
(54) Guo, L.-H.; Facci, J. S.; McLendon, G.; Mosher, R. *Langmuir* **1994**, *10*, 4588−4593.
(55) Moncelli, M. R.; Herrero, R.; Becucci, L.; Guidelli, R. *Biochim. Biophys. Acta, Bioenerg.* **1998**, *1364*, 373−384.
(56) Forouzan, F.; Bard, A. J.; Mirkin, M. V. *Isr. J. Chem.* **1997**, *37*, 155−163.
(57) Schiller, S. M.; Naumann, R.; Lovejoy, K.; Kunz, H.; Knoll, W. *Angew. Chem., Int. Ed.* **2003**, *42*, 208−211.
(58) Vockenroth, I. K.; Atanasova, P. P.; Long, J. R.; Jenkins, A. T. A.; Knoll, W.; Köper, I. *Biochim. Biophys. Acta, Biomembr.* **2007**, *1768*, 1114−1120.
(59) Zazpe, R.; Hibert, C.; O'Brien, J.; Lanyon, Y. H.; Arrigan, D. W. M. *Lab Chip* **2007**, *7*, 1732−1737.
(60) Steinem, C.; Janshoff, A.; Ulrich, W.-P.; Sieber, M.; Galla, H.-J. *Biochim. Biophys. Acta, Biomembr.* **1996**, *1279*, 169−180.
(61) Tien, H. T.; Ottova, A. L. *Electrochim. Acta* **1998**, *43*, 3587−3610.
(62) Legiň, M.; Laputková, G.; Sabo, J.; Vojcíková, L. *Physiol. Res.* **2007**, *56* (Suppl. 1), S85−S91.
(63) Ziegler, W.; Gaburjáková, J.; Gaburjáková, M.; Sivák, B.; Rehacek, V.; Tvarozek, V.; Hianik, T. *Colloids Surf., A* **1998**, *140*, 357−367.
(64) Weiss, S.; Millner, P.; Nelson, a *Electrochim. Acta* **2005**, *50*, 4248−4256.
(65) Plant, A. L.; Gueguetchkeri, M.; Yap, W. *Biophys. J.* **1994**, *67*, 1126−1133.
(66) Jeuken, L. J. C.; Bushby, R. J.; Evans, S. D. *Electrochem. Commun.* **2007**, *9*, 610−614.
(67) Dilger, J.; McLaughlin, S.; McIntosh, T.; Simon, S. *Science* **1979**, *206*, 1196−1198.
(68) Naumowicz, M.; Petelska, A. D.; Figaszewski, Z. A. *Electrochim. Acta* **2009**, *54*, 1089−1094.
(69) Abou-Seif, M. A. M. *Ann. Clin. Biochem.* **1997**, *34*, 645−6650.
(70) Diao, P.; Guo, M.; Jiang, D.; Jia, Z.; Cui, X.; Gu, D.; Tong, R.; Zhong, B. *J. Electroanal. Chem.* **2000**, *480*, 59−63.
(71) Protsailo, L. V.; Fawcett, W. R. *Electrochim. Acta* **2000**, *45*, 3497−3505.
(72) Marcus, R. A.; Sutin, N. *Biochim. Biophys. Acta, Rev. Bioenerg.* **1985**, *811*, 265−322.
(73) Edwards, P. P.; Gray, H. B.; Lodge, M. T. J.; Williams, R. J. P. *Angew. Chem., Int. Ed.* **2008**, *47*, 6758−6765.
(74) James, D. K.; Tour, J. M. *Chem. Mater.* **2004**, *16*, 4423−4435.
(75) Fettiplace, R.; Andrews, D. M.; Haydon, D. A. *J. Membr. Biol.* **1971**, *5*, 277−296.
(76) Aguiar, F. A.; Campos, R.; Wang, C.; Jitchati, R.; Batsanov, A. S.; Bryce, M. R.; Kataky, R. *Phys. Chem. Chem. Phys.* **2010**, *12*, 14804−14811.
(77) Campuzano, S.; Pedrero, M.; Montemayor, C.; Fatás, E.; Pingarrón, J. M. *J. Electroanal. Chem.* **2006**, *586*, 112−121.
(78) Tsionsky, M.; Bard, A. J.; Mirkin, M. V. *J. Am. Chem. Soc.* **1997**, *119*, 10785−10792.